

## RESEARCH PAPER

# A role for a cell wall localized glycine-rich protein in dehydration and rehydration of the resurrection plant *Boea hygrometrica*

L. Wang<sup>1</sup>, H. Shang<sup>1</sup>, Y. Liu<sup>2</sup>, M. Zheng<sup>1</sup>, R. Wu<sup>1</sup>, J. Phillips<sup>3</sup>, D. Bartels<sup>2,3</sup> & X. Deng<sup>1,2</sup>

<sup>1</sup> Key Laboratory of Photosynthesis and Molecular Physiology, Research Center of Plant Molecular and Developmental Biology, Institute of Botany, Chinese Academy of Sciences, Beijing, China

<sup>2</sup> Department of Plant Breeding and Genetics, Max Planck Institute for Plant Breeding Research, Cologne, Germany

<sup>3</sup> IMBIO (Molekulare Physiologie und Biotechnologie der Pflanzen), University of Bonn, Bonn, Germany

## Keywords

*Boea hygrometrica*; cell wall; Fourier transform infrared spectroscopy; glycine-rich protein; resurrection plant.

## Correspondence

X. Deng, Institute of Botany, Chinese Academy of Sciences, Beijing, China.  
E-mail: deng@ibcas.ac.cn

## Editor

J. Sparks

Received: 3 August 2008; Accepted: 8 December 2008

doi:10.1111/j.1438-8677.2008.00187.x

## ABSTRACT

The acquisition of desiccation tolerance in dicotyledonous angiosperms requires the induction of a co-ordinated programme of genetic and biochemical processes during drying and the adaptive mechanisms are primarily protoplasmic in nature. Recent studies have shown that changes in cell wall structure and composition are also important for recovery after drying, however, the molecular mechanisms that underpin these adaptive responses are largely unknown. Here, the desiccation-tolerant plant *Boea hygrometrica* was used as a model system to investigate the changes in gene expression and cell wall adaptation that take place during extreme dehydration. A cDNA macroarray analysis of dehydration-inducible genes led to the identification of a gene encoding a glycine-rich protein (*BhGRP1*). The corresponding transcript was up-regulated during drying in *B. hygrometrica* leaves. *In silico* analysis revealed that *BhGRP1* is targeted to the cell wall and this was confirmed *in planta*. Morphological changes in the cell wall architecture were also observed during the process of drying and re-watering. Concomitant with this observation, cell wall profiling by Fourier transform infrared spectroscopy indicated that protein levels increased upon desiccation and remained broadly similar upon re-watering. These findings suggest that the deposition of *BhGRP1* may play a role in cell wall maintenance and repair during dehydration and rehydration in *B. hygrometrica*.

## INTRODUCTION

Desiccation tolerance is primarily protoplasmic in nature (Bewley 1979). The mechanisms that prevent cellular damage, maintain physiological integrity and mobilise repair upon rehydration are largely a result of the properties of the cellular contents. There are, however, important structural features that are also thought to contribute to the mechanics of desiccation tolerance, which are related to the cell wall (Vicré *et al.* 2004; Moore *et al.* 2008a).

Little is known about the cell wall of desiccation tolerant plants. A structural adaptation that has been reported for desiccation tolerant liverworts is a high degree of cell

wall extensibility (Proctor 1999). Liverworts colonize intermittently desiccated habitat, therefore rapid changes in cell volume take place. The elastic nature of the cell wall is thought to play a role in cell water relations (Proctor 1999). More recently a relatively high degree of wall flexibility was shown for the desiccation tolerant plant *Craterostigma plantagineum* and *Myrothamnus flabellifolia* (Jones & McQueen-Mason 2004; Moore *et al.* 2008b).

Few studies have been performed on examining the effects of drought on higher plant cell walls. Structural studies of resurrection plants such as *Craterostigma wilmsii*, *Eragrostis nindensis*, *M. flabellifolia* and *Selaginella lepidophylla* have revealed that cell walls are highly folded

in the dried state (Thomson & Platt 1997; Vicré *et al.* 1999, 2004; Vander Willigen *et al.* 2003). The folding of the cell wall allows the plasma membrane to remain firmly attached to the wall while the cell loses water. Biochemical modifications of the cell wall in *C. wilmsii* and *Myrothamnus flabellifolius* have been observed during dehydration and rehydration (Vicré *et al.* 2004; Moore *et al.* 2006), leading to changes in tensile strength that may prevent total collapse of the walls in the dry tissue and avoid rapid expansion upon rehydration; however, the molecular genetics that underlies cell wall mechanical properties is largely unknown.

*Boea hygrometrica* is a desiccation tolerant angiosperm native to China (Deng *et al.* 1999). Studies of the photosynthetic apparatus reveal that *B. hygrometrica* does not lose chlorophyll during desiccation, indicating that the species is homiochlorophyllous. Furthermore, the carotenoid content increases during dehydration, which is thought to play a role in the recovery of photosynthetic activity during rehydration (Deng *et al.* 2003). The most striking feature of *B. hygrometrica*, however, is that a single detached leaf or leaf disc can survive at least one cycle of dying and rehydration, a property that is restricted to a subset of desiccation tolerant plants (Deng *et al.* 2003; Jiang *et al.* 2007). Previous studies have also shown that changes in gene expression and protein accumulation accompany changes in water content (Deng *et al.* 1999; Jiang *et al.* 2007).

In this work, we report that a gene encoding a glycine-rich protein (BhGRP1) was identified among genes that are induced by dehydration in detached leaves of *B. hygrometrica* via a cDNA macroarray approach. Glycine-rich proteins (GRPs) compose a large family of heterogenous proteins that contain high proportions of glycine residues, up to 60–70% of the total amino acid residues (Sachetto-Martins *et al.* 2000). One class of GRPs contain a RNA-binding domain and are involved in the regulation of RNA processing inside the nucleus or are similar to animal cytokeratins (Mousavi & Hotta 2005), while another class of GRPs are targeted to the extracellular matrix and function as structural components of plant cell walls (Sachetto-Martins *et al.* 2000; Ringli *et al.* 2001). Many GRPs are induced by external influences such as wounding, hormone treatment, low temperature and water or ozone stress. Water stress induces several GRP genes in both resurrection and non-resurrection plants (de Oliveira *et al.* 1990; Neale *et al.* 2000). Here the cellular localization and expression profile of BhGRP1 were investigated along with the architectural and compositional changes of the cell wall of *B. hygrometrica* leaves in the adaptation to extreme dehydration. Evidence is provided to support the theory that, in addition to changes in the cytoplasm, membranes and sub-cellular organelles, reversible and non-reversible alterations to the cell wall architecture play an important role in desiccation tolerant angiosperm species, and cell wall structural proteins function in this tolerance mechanism.

## MATERIAL AND METHODS

### Plant materials, stress treatment, and estimation of relative water content

Plants of *B. hygrometrica* (Bunge) R. Br. were collected from shallow rock crevices at E116°/N40° in a suburb of Beijing and grown under greenhouse conditions (25 °C, 16 h/8 h light period, with regular irrigation). Dehydration and rehydration treatments, as well as relative water content (RWC) measurements were carried out as described previously (Jiang *et al.* 2007). *Nicotiana benthamiana* was grown under the same greenhouse conditions as described above.

### cDNA collection and preparation of macroarray filters

4562 *B. hygrometrica* clones from a cDNA library constructed from dehydrated leaves using a ZAP-cDNA<sup>®</sup> Library Construction Kit (Stratagene, La Jolla, CA, USA), together with a constitutively expressed actin cDNA clone and spiking controls including GUS, desmin and neblin (Bellin *et al.* 2002), were amplified by PCR (36 cycles, denaturing at 94 °C for 45 s, annealing at 55 °C for 30 s and extending at 72 °C for 90 s) in a 96-well format with approximately 100 ng of plasmid DNA as template, using M13 forward and reverse primers. The PCR fragments were spotted onto positively charged nylon membranes (Amersham Biosciences, Freiburg, Germany) using a BioGrid robot (BioRobotics Ltd, Cambridge, UK) as described by Hoheisel *et al.* (1993).

### Macroarray hybridizations and data analysis

Membranes were pre-hybridized for 2 h in 0.5 M sodium phosphate pH 7.2, 7% (w/v) SDS, 1 mM ethylenediaminetetraacetic acid (EDTA) pH 8.0 and 100 µg·ml<sup>-1</sup> salmon sperm DNA, as described by Hoheisel *et al.* (1993). Filters were hybridized with <sup>33</sup>P-labelled cDNAs derived from poly (A)<sup>+</sup> RNA isolated from untreated and dehydrated plants and washed as described previously (Deng *et al.* 2006). Filters were exposed to a phosphor screen (Kodak, Rochester, NY, USA) for 18 h. Hybridisation signals were obtained with a Storm scanner (Amersham Pharmacia Biotech, USA) and signal intensity was quantified using Array Vision software (Imaging Research Inc., Canada). Background due to non-specific binding of probes to the membrane was subtracted from the signal intensity of each spot. Global normalization was adopted for normalizing the difference of signal intensity of each nylon filter. The intensity was calculated as the ratio of each signal to the average intensity of controls. Data were obtained from four independent experiments and were statistically analysed using Array Stat software (Imaging Research Inc.). Signals differing more than 2.5-fold in independent hybridization experiments were considered to be significantly up- or down-regulated.

### Total RNA extraction and quantitative RT-PCR

Total RNA was extracted according to Chomczynski & Sacchi (1987). Briefly, the RNA extraction buffer contained 4 M guanidinium thiocyanate, 25 mM sodium citrate, pH 7.0; 0.5% sarcosyl, 0.1 M 2-mercaptoethanol. The semi-quantitative RT-PCR was performed according to a method adapted from Meadus (2003). Briefly, 2 µg total RNA were heated to 70 °C for 5 min and then reverse transcribed using M-MLV reverse transcriptase (Promega, USA) in combination with random primers for 60 min at 42 °C in a 25 µl volume. PCR was performed on cDNA samples (1 µl of a 1:5 dilution) using *rTaq* polymerase (TaKaRa, Japan). The *BhGRP1* (Genbank accession no. EU003996) gene specific primers used are 5'-CGCCAA GTTTCAGAGGTAGAGAGA-3' and 5'-TCCATGGCGTC GGTGGTCTCAG-3'. The *BhLEA1* (Genbank accession no. EU122334) gene specific primers are 5'-GGAATT CAAGATGCAAGCTGTGA-3' and 5'-GCTCGAGTCATT TCAGGCCATGG-3'; the 18S rRNA was amplified using the primer combination 5'-TTGTGTTGGCTTCGGGATC GGAGTAAT-3' and 5'-TGCACCACCACCCATAGAATC AAGAA-3' as a constitutive control. The linear range of detection for each transcript was monitored and samples run for 25 cycles for *BhGRP1*; 32 cycles for *BhLEA1* and 18 cycles for 18S rRNA were compared. Three repetitions were performed for each sample. Band intensity was assessed using AlphaEaseFc 4.0 (Alpha Innotech, USA). Intensities of bands corresponding to *BhGRP1* and *BhLEA1* mRNA transcripts were normalized to 18S rRNA levels. All statistical analyses were conducted with SPSS 11.5 (SPSS, USA). The significance level was set at  $P < 0.05$ .

For quantitative real-time PCR, total RNAs were isolated using TRIzol Reagent (Invitrogen, USA) according to the manufacturer's protocol. RNase-free DNase (TaKaRa) was used to remove genomic DNA contamination. Aliquots of RNA (1 µg) were reverse-transcribed using the RevertAid™ First Strand cDNA Synthesis Kit (Fermentas, Lithuania) according to the manufacturer's instructions. Quantitative real-time PCR analyses were performed on an ABI 7500 Fast Real-time PCR System (Applied Biosystems, USA). PCR was conducted in a final volume of 20 µl containing the following: SYBR Green Realtime PCR Master Mix (TaKaRa) and 0.25 µM of each primer, using the first strand cDNA as the PCR template. Amplification conditions were as follows: 95 °C for 10 s, 40 cycles of 95 °C for 5 s and 62 °C for 34 s. Primers for *BhGRP1* were 5'-TTCTTGGCCTTTTGTGGCC-3' and 5'-CGTTTCCTTCTCTGCGTCAATG-3'; and for 18S rRNA were 5'-CGGCTACCACATCCAAGGAA-3' and 5'-GCTGGAATTACCGCGGCT-3'. The *BhGRP1* expression data are presented as relative expression units after normalization to the 18S rRNA control using  $2^{-\Delta\Delta CT}$  method. The mean expression values and SD values were calculated from the results of three independent experiments.

### DNA and protein sequence analysis

DNA sequence similarities were determined using the BLAST program (Altschul *et al.* 1990). The phylogenetic tree was constructed with MEGA 3.0 software (Kumar *et al.* 2004) using the Neighbour-Joining method. The stability of internal nodes was assessed by bootstrap analysis with 1000 replicates. Signal peptide prediction was conducted using SignalP V3.0 (<http://www.cbs.dtu.dk/services/SignalP/>). The hydropathic index was calculated according to the Kyte-Doolittle scale (<http://www.expasy.org/tools/protscale.html>). Secondary structure prediction was performed using PredictProtein (<http://www.predictprotein.org>).

### GFP fusion protein expression in *N. benthamiana* and laser scanning confocal microscopy

The *BhGRP1* (GenBank accession no. EU003996) open reading frame was amplified using gene specific primers (described in 'RNA extraction and quantitative real-time PCR'). The resulting PCR fragment was then subcloned in frame with the 5'-terminus of the GFP coding sequence in a vector containing the double *CaMV* 35S promoter with a duplicate transcriptional enhancer, the tobacco etch virus translational enhancer, and the *CaMV* 35S polyadenylation site (Reichel *et al.* 1996). The entire cassette was subcloned into the pBIN19 vector via the *HindIII* site. The plasmids containing *BhGRP1*-GFP and GFP alone were transiently transformed into *N. benthamiana* leaves via an *Agrobacterium* mediated method (Kapila *et al.* 1997) and the fluorescent GFP signals were visualized using a Zeiss confocal microscope (LSM 510 META) (excitation wavelength:  $480 \pm 20$  nm; emission wavelength:  $510 \pm 20$  nm). Zeiss LSM Image Browser software (version 3.2.0.70) was used for image acquisition.

### Resin embedded samples for light microscopy and transmission electron microscopy

Leaf segments (approx. 5 mm<sup>2</sup>) excised from three different leaves of each water condition were fixed in Karnovsky's fixative (4.0% formaldehyde and 5.0% glutaraldehyde in 0.2 M phosphate buffer, pH 7.2; Karnovsky 1965), followed by post-fixation in 1% (w/v) osmium tetroxide in phosphate buffer. After ethanol dehydration, materials were infiltrated over 4 days and then embedded in the epoxy resin (Spurr 1969). Semi-thin sections (1 µm) and ultra thin sections (approx. 70 nm) were obtained using an ultra microtome (Leica, Germany) with glass knives. Semi-thin sections were stained with toluidine blue (1% Toluidine Blue in 1% borate) and observed with an Axioskop 40 fluorescence microscope (Zeiss, Germany). Ultra thin sections were stained with uranyl acetate and lead citrate (Reynolds 1963) and observed with a JEM-1230 TEM (JEOL, Japan).

### Extraction of cell wall materials

Extraction of cell wall materials was performed according to Alonso-Simón *et al.* (2004). Briefly, about 1 g leaves were ground to a fine powder in liquid nitrogen and homogenized in cold 100 mM potassium phosphate buffer (pH 7.0) on ice. The mixture was vortexed and centrifuged (1000 g, 10 min). This step was repeated four times. The pellet was resuspended in cold redistilled water and centrifuged, which was repeated five times. The resulting pellet was washed three times with acetone, methanol:chloroform (1:1; v/v), followed by three washes with diethylether and then air-dried.

### Fourier transform infrared spectroscopy

The cell wall materials were layered on a barium fluoride window. Spectra were obtained using a MAGNA-IR 750 Fourier transform infrared (FTIR) spectrometer (Nicolet, USA) equipped with a mercury-cadmium-telluride (MCT/A) detector. The spectra were recorded in absorbance mode by accumulating 128 scans with a resolution of 4 cm<sup>-1</sup> in the spectral range of 3800–1200 cm<sup>-1</sup>. Three independent repetitions were conducted on cell wall materials isolated from (i) hydrated, (ii) desiccated and (iii) rehydrated leaves. Principal component analysis

(PCA) was conducted using SIMCA-P 11.5 software (Umetrics, Sweden). The spectra between 1200 and 2000 cm<sup>-1</sup> were subjected to PCA. Binary comparisons were performed between hydrated and dehydrated (H–D), dehydrated and rehydrated (D–R), hydrated and rehydrated (H–R) samples.

## RESULTS

### Identification of a dehydration-responsive glycine-rich protein gene, *BhGRP1*

Plant adaptation to desiccation is likely to occur as a result of changes in gene expression. Expression analysis of 4562 cDNA clones from a library prepared from partially dried leaves was used to identify dehydration inducible genes that encode proteins that function during the resurrection process. Macroarray results showed that most of the samples (around 93% of the total clones) tested were expressed in a range between 2.0 and 0.5 that indicated no response to dehydration. cDNA clones with an expression ratio greater than twofold compared to the control were classified as potentially 'dehydration responsive' and subsequently sequenced. In total 42 cDNA clones were identified, including genes encoding putative cell wall-associated proteins, enzymes in carbohydrates metabolism, LEA (Late

**Table 1.** Genes induced by dehydration identified using macroarray and confirmed by northern analysis.

function group	gene product	clone ID	GenBank hit/function	no. cDNAs clones	array ratio	
					D2:unt	D8:unt
signal pathway	WRKY transcription factor	PA-84	AAW30662, WRKY21 ( <i>Larrea tridentate</i> )	1	3.7	2.8
		C-75	DAA05134, WRKY69 (rice)	1	3.9	2.4
	heat stress transcription factor	OA-41	AAM43804, HSF9 ( <i>Helianthus annuus</i> )	1	5.4	3.5
		J-16	CAC34625 (alfalfa)	3	3.4	3.2
	calcium binding protein	E-46	AAF31151 ( <i>Olea europaea</i> )	1	5.7	3.7
		B-63	P31237 (kiwifruit)	2	2.4	1.6
cell wall associated	glycine-rich protein	10-62	P37703, GRP DC9.1 ( <i>Daucus carota</i> )	1	3.3	3.6
	germin-like protein	Q-8	P92996, GLP5A ( <i>Arabidopsis thaliana</i> )	1	2.4	1.8
	dirigent protein-related	27-70	ABD52112, pDIR1 ( <i>Picea glauca</i> )	1	3.8	2.3
sugar metabolism	galactinol synthase	J-57	CAB51534, GolS-2 ( <i>Ajuga reptans</i> )	3	9.0	7.6
	raffinose synthase	U-91	AAD02832, Q93XK2 (pea seeds)	1	5.5	4.9
	beta-amylase	R-24	P10537 (sweet potato)	2	4.0	3.1
protective proteins	LEA protein	10-47	AAD01541 ( <i>Glycine max</i> )	1	4.5	4.0
		OB-44	AAZ72650 ( <i>Craterostigma plantagineum</i> )	1	2.9	1.9
	heat shock cognate protein	B-56	AAB97316, HSC70-3 ( <i>Spinacia oleracea</i> )	1	3.4	2.6
protein degradation	polyubiquitin	D-36	CAA54603 (tobacco)	1	2.8	2.1
	stress related	7-42	AY224428 (rice)	2	4.0	2.5
		12-43	AAA03020, pSTH-21 ( <i>Solanum tuberosum</i> )	3	2.4	1.8
secondary metabolism	orcinol O-methyltransferase	5-65	AAD38293 (rice)	4	3.2	2.1
		12-28	CAH05083 (Rosa hybrid cultivar 'Kazanlik')	1	3.0	1.5
		B-41	CAC37358 ( <i>Solanum tuberosum</i> )	1	4.9	2.7
unknown proteins	putative membrane protein	23-45	BAC06446, RPP17-2 (rice)	1	2.7	2.0
	C2 domain-containing protein	4-56	AAK30572 ( <i>Brassica napus</i> )	1	3.7	2.6
	expressed protein	U-87	NP563661 ( <i>Arabidopsis thaliana</i> )	1	4.0	3.3
	expressed protein	G-75	AAD51628, PM41 ( <i>Glycine max</i> )	2	2.8	2.3
	putative protein	29-79	no match	4	3.9	5.4

```

1  ATCCAAATTGAAGTGCAAACCTTAAATCTAATATGGGTTACAAAGCAATGTCTTTCTTGGCCCTTTTGTGGCCATAGTCTTCTCATTTCCTCGGAGGT 100
      M G Y K A I V F L G L F V A I V L L I S S E V
101 GGGCGCTAGAGAATTGGCTGAGACCACCGACGCCATTGACGCAGAGAAGGAAACGGAGGCAACTGAAGATGGTCGAGGTGGATATAATGGATATGGCCGC 200
      G A R E L A E T T D A I D A E K E T E A T E D G R G G Y N G Y G G
201 GGTCGAGGTGGATATGGAGGATATGGCCGGGTCGAGGAGGATATGGACGCGGCGGAGGTGGATACGGAGGTGGTCACGGTGGATACGGAGGTGGTGGCC 300
      G R G G Y G G Y G G G R G G Y G R G R G G Y G G G H G G Y G G G H
301 ACGGTGGATACGGACGTGGCCGAGGTGGACATGGAGGAGGTGGCCACGGTGGATACGGAGGAGGACGGGTGGACACGGCCGGAAGCTGTGGATCCCGA 400
      G G Y G R G R G G H G G G G H G G Y G G G R G G H G G E A V D P D
401 CTTTGTGAAGCCGAAACTCACAACCTAAACTGCAAATCCAGCCCAAGACATATATATACTCAGATAAAATAAAGAATTGCATGGATGAATTATCTGA 500
      F V E A E T H N *
501 CATCTGTTCATGTAATAATAACACTGTCCGATGTGAAACCTTGTGCACATATCAGTTATCAGATGTTGTTTCGAGTTTGATTATGTAAGATGTTCTGTGGT 600
601 TGATATAC 608

```

Fig. 1. Nucleotide sequence of *BhGRP1*. The predicted protein sequence is shown beneath the nucleotide sequence.

Embryogenesis Abundant) proteins, and proteins involved in signal transduction pathways and proteins with unknown function (Table 1). Among them, a 608 bp cDNA (clone ID 10-62, Table 1) was identified to be induced 3.3- to 3.6-fold upon dehydration. This cDNA fragment contained a 396 bp open reading frame (ORF), a 32 bp 5'-untranslated region and a 180 bp 3'-untranslated region terminating in a poly (A) tail (Fig. 1). The open reading frame encoded a gene product with a high degree of similarity to glycine-rich proteins (Genbank accession no. EU003996, designated *BhGRP1*). To validate the expression pattern of *BhGRP1*, semi-quantitative RT-PCR was performed (Fig. 2A). *LEA* gene has been widely reported in response to water stress, therefore the dehydration responsive *BhLEA1* gene (Genbank accession no. EU122334; Liu *et al.* 2008) was also included as a control to qualify the RNA samples. Results from three independent experiments showed that, compared with the hydrated sample, the *BhGRP1* mRNA was significantly up-regulated upon dehydration (1.6- to 2.4-fold,  $P < 0.05$ ) and rehydration (twofold,  $P < 0.05$ ). This observation was further validated using quantitative real-time PCR (Fig. 2B). A 5.2-fold increase in the partially dehydrated sample, a 3.4-fold increase in the fully dehydrated sample, and a 4.1-fold increase in the rehydrated sample in *BhGRP1* transcripts were observed in comparison with the hydrated control. These data demonstrate that *BhGRP1* is induced by dehydration and thus may play a role in the adaptation to dehydration.

#### *BhGRP1* sequence and phylogenetic analysis

The *BhGRP1* ORF encodes a predicted protein of 131 amino acids, with a 45% glycine-rich region between amino acids 47 and 117 comprised of GX, GGX, GGGX, and GGGGX motifs. The glycine-rich region is composed exclusively of three other types of hydrophilic amino acid residues: arginine, histidine or tyrosine. An N-terminal cleavable signal peptide (predicted by SignalP V3.0) was recognised in *BhGRP1* that shares homology with a cell wall protein from tomato (Domingo *et al.* 1999). The existence of the extracellular signal peptide and the absence of a RNA binding domain indicated that *BhGRP1* is likely to function in the cell wall.

A phylogenetic tree comprising of *BhGRP1* and cell wall associated GRPs from rice, *Arabidopsis*, saltbush, tomato, loblolly pine, alfalfa, bean and the desiccation tolerant grass *Sporobolus stapfianus* was constructed (Fig. 3A). Analysis of the tree revealed a close relationship between *BhGRP1* and *AtGRP3* (S47409, Fig. 3B), a drought-induced GRP protein from *Arabidopsis*. *AtGRP3* is capable of interacting with the extracellular domain of the cell wall-associated receptor protein kinase WAK1 to activate downstream processes *in planta* (de Oliveira *et al.* 1990; Anderson *et al.* 2001; Park *et al.* 2001).

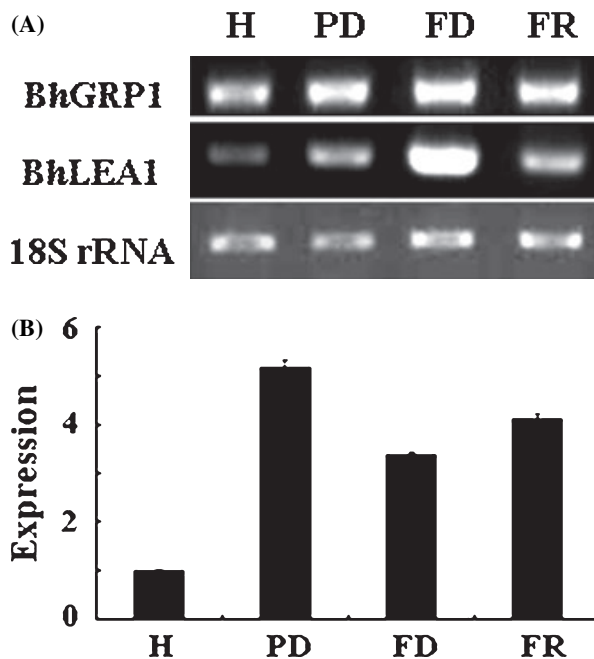
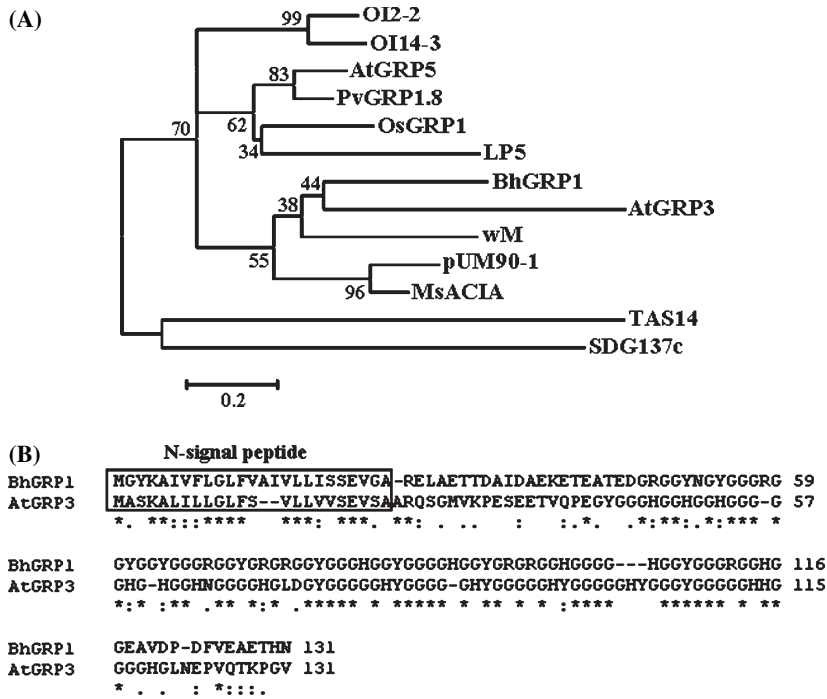
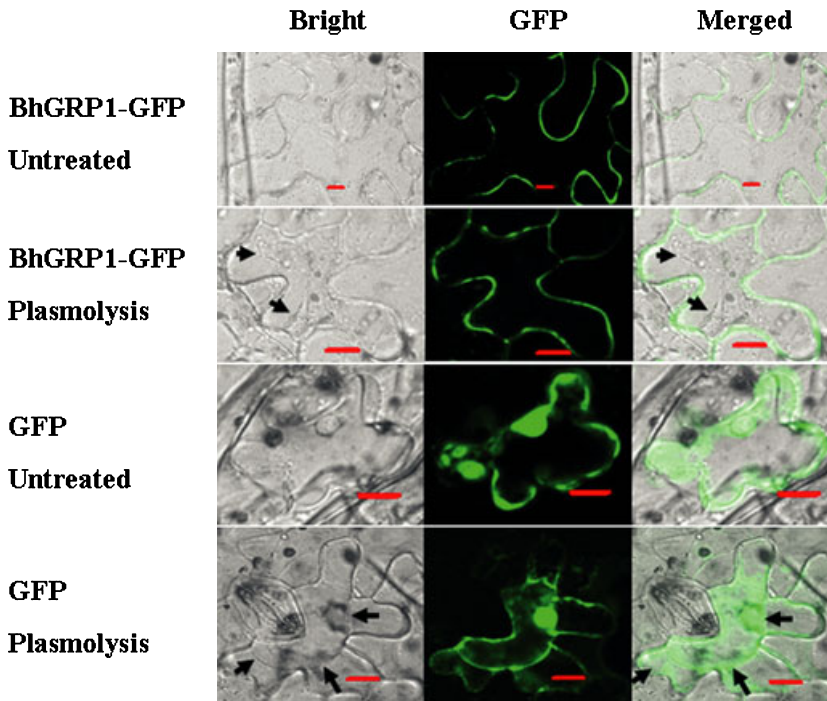


Fig. 2. Expression analysis of *BhGRP1* in response to dehydration and rehydration. A: Semi-quantitative RT-PCR analysis; B: Quantitative real-time PCR analysis of *BhGRP1* expression. The *BhGRP1* gene was amplified with cDNAs reversely transcribed from total RNA isolated from hydrated (H; RWC = 100%), partially (PD; RWC = 40%) and fully dehydrated (FD; RWC < 5%) and fully rehydrated (FR; RWC ~ 100%) leaves. 18S rRNA and *BhLEA1* was amplified as constitutive and dehydration responsive controls respectively.



**Fig. 3.** Phylogenetic tree (A) and sequence alignment (B) of BhGRP1 and water stress-associated, cell wall glycine-rich proteins. An unrooted phylogram was generated with the protein sequences of BhGRP1 (EU003996) from *Boea hygrometrica*, AtGRP3 (S47414) from *Arabidopsis thaliana*, OI2-2 (T64462) and OI14-3 (T64463) from saltbush, wM (X55688) and TAS14 (X51904) from tomato, pUM90-1 (AAA32653) and MsACIA (L03708) from alfalfa, PvGRP1.8 (X13596) from bean, OsGRP1 (P25074) from rice, LP5 (AF013805) from loblolly pine, and SDG137c (AJ242802) from *Sporobolus stapfianus*. Bootstrap values from 1000 replications for each branch are shown.



**Fig. 4.** Cell wall localization of BhGRP1. The BhGRP1-GFP fusion protein was transiently expressed for 48 h in *Nicotiana benthamiana* leaves using an *Agrobacterium* mediated system. A GFP vector was transformed in parallel as a control. Epidermal strips of transformed leaves were isolated and incubated in redistilled water (Untreated) or 0.8 M mannitol solution (Plasmolysis) for 5 min before observation. GFP fluorescence was visualised using confocal microscopy. The arrows show the regions undergoing plasmolysis. Scale bar: 10  $\mu$ m.

#### BhGRP1 is targeted to the plant cell wall

To test whether the BhGRP1 protein is targeted to the cell wall, a GFP fusion was constructed. The construct was expressed in *N. benthamiana* and analysed using confocal laser scanning microscopy. In contrast to a GFP

control, the BhGRP1-GFP fusion protein signal was restricted to the cell borders (Fig. 4). When the plasma membrane was detached from the cell wall through plasmolysis by incubating the cells in 0.8 M mannitol, the BhGRP1-GFP fusion protein signal was detected at the cell wall (Fig. 4, BhGRP1-GFP plasmolysis), while the

GFP control signal was found throughout the cell (Fig. 4, GFP plasmolysis). The cell wall localization of BhGRP1-GFP fusion protein was demonstrated in the merged images, where the fluorescence signal is distinct from the detached plasma membrane.

#### Reversible cell wall folding during dehydration and rehydration

*Boea hygrometrica* plants have adapted to dry and wet seasons in China. In the desiccated state, vegetative tissues are shrunken and dormant, however, when water is available, tissues hydrate, expand and recover viability (Deng *et al.* 2003; Jiang *et al.* 2007). Histological analysis was applied to examine the leaf ultrastructure during the dehydration/rehydration cycle. Transverse semi-thin sections revealed that the hydrated leaves (RWC = 100%) were composed of large upper epidermal cells, several layers of palisade and spongy parenchyma cells and a

layer of smaller, rounded lower epidermal cells (Fig. 5A). Transmission electron microscopy revealed that all mesophyll cells exhibited smooth cell walls, large central vacuoles, and defined nuclei (Fig. 5F and K). Upon dehydration, water loss was rapid: approximately 60% of the water was lost within 2 h, and <5% remained after 48 h. Leaf tissues dramatically reduced in size and folded inwards. Transverse sections from partially and fully dehydrated leaves revealed a reduction in cellular volume and intercellular space (Fig. 5B and C). The cytoplasm became compact upon dehydration as indicated by the increased electron density (Fig. 5G and H). Cell wall folding and shrinkage occurred simultaneously, most noticeably in desiccated cells (Fig. 5L and M). Cell wall folding occurred predominantly along the latitudinal sides of the upper epidermis and palisade cells, while the longitudinal walls were broadly unaffected, which gave rise to a 'concertina' effect (Fig. 5G and H). Plasmolysis within mesophyll cells was

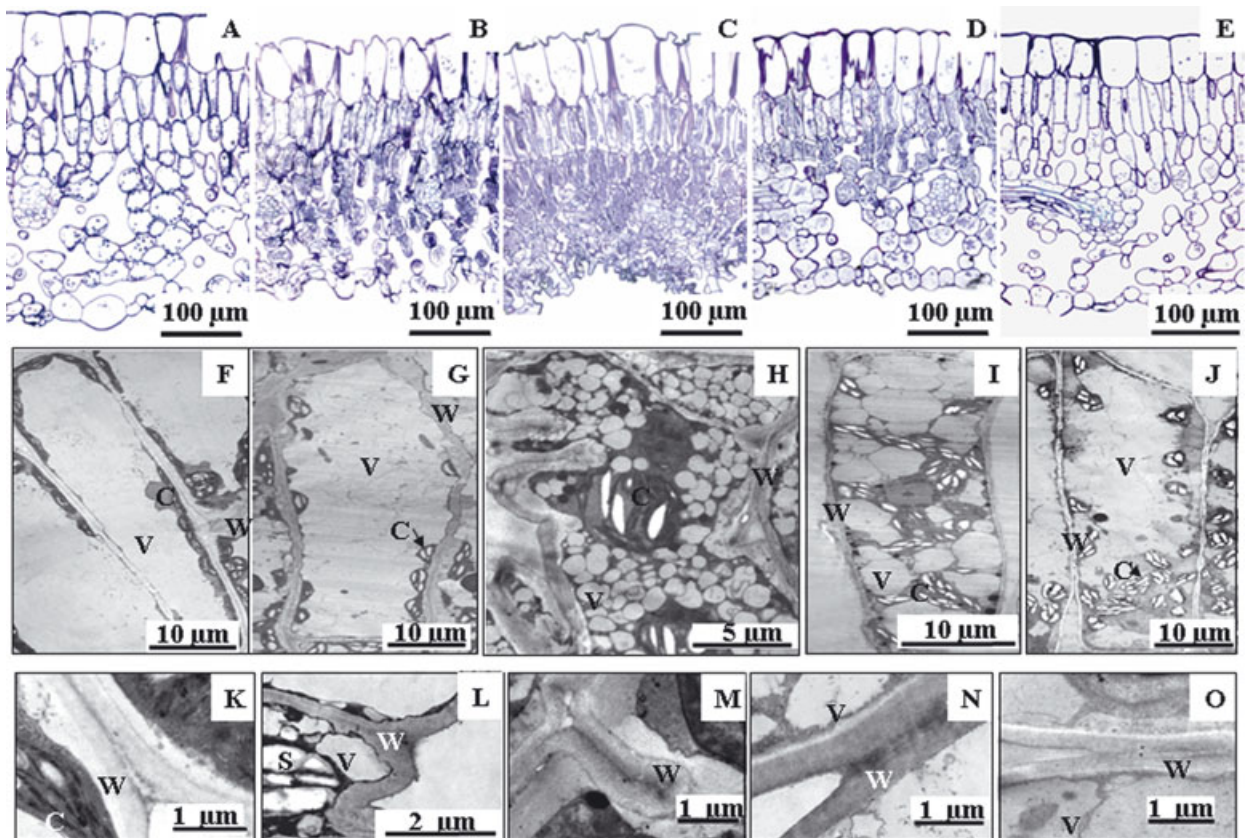


**Fig. 5.** Structure changes of *Boea hygrometrica* leaves during the process of dehydration and rehydration. A–E: Effect of dehydration and rehydration on the structure of *B. hygrometrica* leaves. F–J: Ultra-structural analysis of *B. hygrometrica* palisade cells at different relative water contents. K–O: Effect of dehydration and rehydration on the cell wall of mesophyll cells of *B. hygrometrica* leaves. Leaves from untreated plants (RWC = 100%, A, F, K) were dried under  $45 \pm 5\%$  relative humidity and moderate illumination at  $25^\circ\text{C}$  to a relative water content of  $\sim 40\%$  (partially dehydrated, B, G, L) and  $<5\%$  (fully dehydrated, C, H, M). Desiccated leaves were subsequently rehydrated for 8 and 48 h to reach RWCs of  $\sim 75\%$  (partially rehydrated) (D, I, N) and  $\sim 100\%$  (fully rehydrated) (E, J, O). Semi-thin sections ( $1\ \mu\text{m}$ , A–E) were stained with toluidine blue. Ultra-thin sections ( $70\ \text{nm}$ , F–J; K–O) were stained with uranyl acetate and lead citrate and viewed using a transmission electron microscope. A scale bar is indicated in each panel. C, chloroplast; W, cell wall; S, starch grain; V, vacuole.

barely visible even in the desiccated leaves (Fig. 5G and H) because the central vacuole disappeared and was replaced by numerous smaller vacuoles. Chloroplasts and nuclei appeared irregularly shaped in the mesophyll cells, although the membranes appeared intact (Fig. 5G and H).

After 8–48 h of rehydration, leaves broadly regained the initial relative water content (about 75–100% of the original level). Changes that occurred during dehydration were partially reversed: the upper epidermis and mesophyll cells assumed their original size and shape (Fig. 5D and E). Spaces among mesophyll cells were visible and the compacted cytoplasmic matrix diminished, as indicated by the low electron density (Fig. 5I and J). The cell wall was no longer folded (Fig. 5N and O), mid-sized vacuoles appeared and chloroplasts reverted to the original elliptical shape at this stage (Fig. 5I and J).

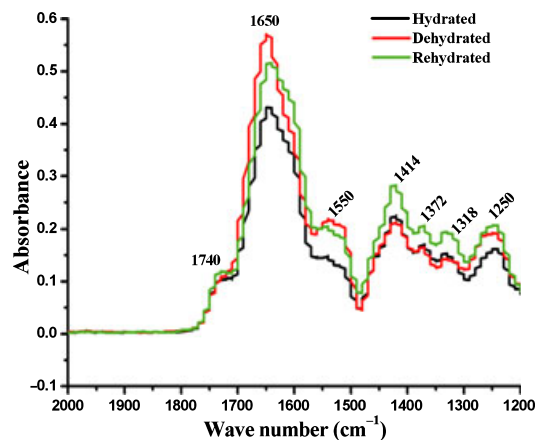
#### Alterations in cell wall composition caused by dehydration and rehydration

Fourier transform infrared (FTIR) spectroscopy was used to study the chemical composition of the leaf cell wall. The FTIR spectra corresponded to the following chemical

groups (absorption maxima/range given in brackets): saturated esters (1740  $\text{cm}^{-1}$ ; Morikawa *et al.* 1978), amide bonds of protein (1650 and 1550  $\text{cm}^{-1}$ ; Sutherland 1952), carboxylic acid groups (1600 and 1414  $\text{cm}^{-1}$ ; Morikawa *et al.* 1978), phenolic groups (1620 and 1515  $\text{cm}^{-1}$ ; McCann *et al.* 1994) and octadecyl octadecanoate stretches (1372, 1318 and 1250  $\text{cm}^{-1}$ ; Zeier & Schreiber 1999).

Changes in the cell wall composition were determined by comparing peak height from the different spectra. Data obtained from hydrated (RWC = 100%), dehydrated (RWC < 5%) and rehydrated (RWC = ~100%) leaf samples are shown in Fig. 6. Differences in spectra between the hydrated and dehydrated samples were evident at 1650 and 1550  $\text{cm}^{-1}$  (Fig. 6). These characteristics correspond to amide I and amide II groups, indicating an increase in protein content in dehydrated leaves. These signals decreased slightly in rehydrated samples, but remained higher than in the hydrated samples, demonstrating that cell wall proteins are accumulated after dehydration, and that the dehydration-induced accumulation of proteins is not reversed upon rehydration.

The intensity peaks at 1740 and 1414  $\text{cm}^{-1}$  corresponded to saturated esters and carboxylic acids were similar in hydrated and dehydrated leaves, but higher in rehydrated leaves (Fig. 6). These observations indicate



Wave number/ chemical group	Absorption height						
	1740 $\text{cm}^{-1}$ Saturated esters	1650 $\text{cm}^{-1}$ Amide II	1550 $\text{cm}^{-1}$ Amide I	1414 $\text{cm}^{-1}$ Carboxylic acids	1372 $\text{cm}^{-1}$	1318 $\text{cm}^{-1}$	1250 $\text{cm}^{-1}$ Octadecyl octadecanoate
Hydrated	0.086 ± 0.019	0.425 ± 0.023	0.149 ± 0.009	0.216 ± 0.041	0.180 ± 0.039	0.151 ± 0.039	0.179 ± 0.053
Dehydrated	0.083 ± 0.004	0.569 ± 0.044	0.191 ± 0.032	0.218 ± 0.037	0.181 ± 0.046	0.152 ± 0.045	0.192 ± 0.041
Rehydrated	0.110 ± 0.001	0.507 ± 0.019	0.202 ± 0.036	0.271 ± 0.018	0.207 ± 0.011	0.188 ± 0.012	0.207 ± 0.009

**Fig. 6.** *Boea hygrometrica* leaf cell wall composition changes as a result of dehydration and rehydration. Fourier transform infrared (FTIR) spectra were obtained from cell wall samples extracted from untreated (black; RWC = 100%), fully dehydrated (red; RWC < 5%) and fully rehydrated (green; RWC ~ 100%) leaves. The experiments were repeated three times and the average values were used to generate the final FTIR spectra [x-axis: wave number ( $\text{cm}^{-1}$ ); y-axis: absorbance].

that both esterified and de-esterified pectins are increased in rehydrated leaves. The peaks at 1372, 1318 and 1250  $\text{cm}^{-1}$  correspond to octadecyl octadecanoate (Zeier & Schreiber 1999), indicating that wax- or suberin-like aliphatic compounds were also increased in rehydrated leaves. No differences were detected in lignin or monolignols among the hydrated, dehydrated and rehydrated leaves, as inferred from the unchanged absorbance levels at 1505 or 1595  $\text{cm}^{-1}$  (Fig. 6).

Principal component analysis (PCA) was conducted to further analyse the differences among the spectra of hydrated, dehydrated and rehydrated samples in the range between 1200 and 2000  $\text{cm}^{-1}$ , the region where most variation occurred. Binary comparisons were performed between hydrated and dehydrated (H–D), dehydrated and rehydrated (D–R), hydrated and rehydrated (H–R) samples. Scores plots of PC1 against PC2 showed differentiation among these samples (Fig. 7A). For each case, PC1 and PC2 can explain more than 80% of the variance and separate these spectra. Furthermore, the impacts of each variable (wave number) to each principal component on this clustering were calculated and represented in the corresponding 'loadings plot' (Fig. 7B). The plots indicated that this differentiation is likely to reflect compositional

impacts of the effect of water status changes on protein, pectin and wax/suberin. The major contributions to spectral variation between hydrated and dehydrated leaf cell walls were proteins, represented by the amide I band at 1650  $\text{cm}^{-1}$  and the amide II band at 1550  $\text{cm}^{-1}$ ; the major contributions to spectral variation between desiccated and rehydrated leaf cell walls were de-esterified pectins represented by the carboxylic acids band at 1414  $\text{cm}^{-1}$ , wax- or suberin-like aliphatic compounds represented by the octadecyl octadecanoate bands at 1372, 1318  $\text{cm}^{-1}$ ; and the major contributions to spectral variation between hydrated and rehydrated leaves was the amide I band at 1650  $\text{cm}^{-1}$ , indicating an increase in cell wall proteins in response to dehydration that was not fully reversed by rehydration.

## DISCUSSION

The work presented here shows the identification of dehydration responsive cDNAs encoding putative gene products belonging to eight functional groups using an array-based differential gene expression screening procedure. Of the candidate cDNA clones, the putative glycine-rich protein gene, *BhGRP1*, was further characterized.

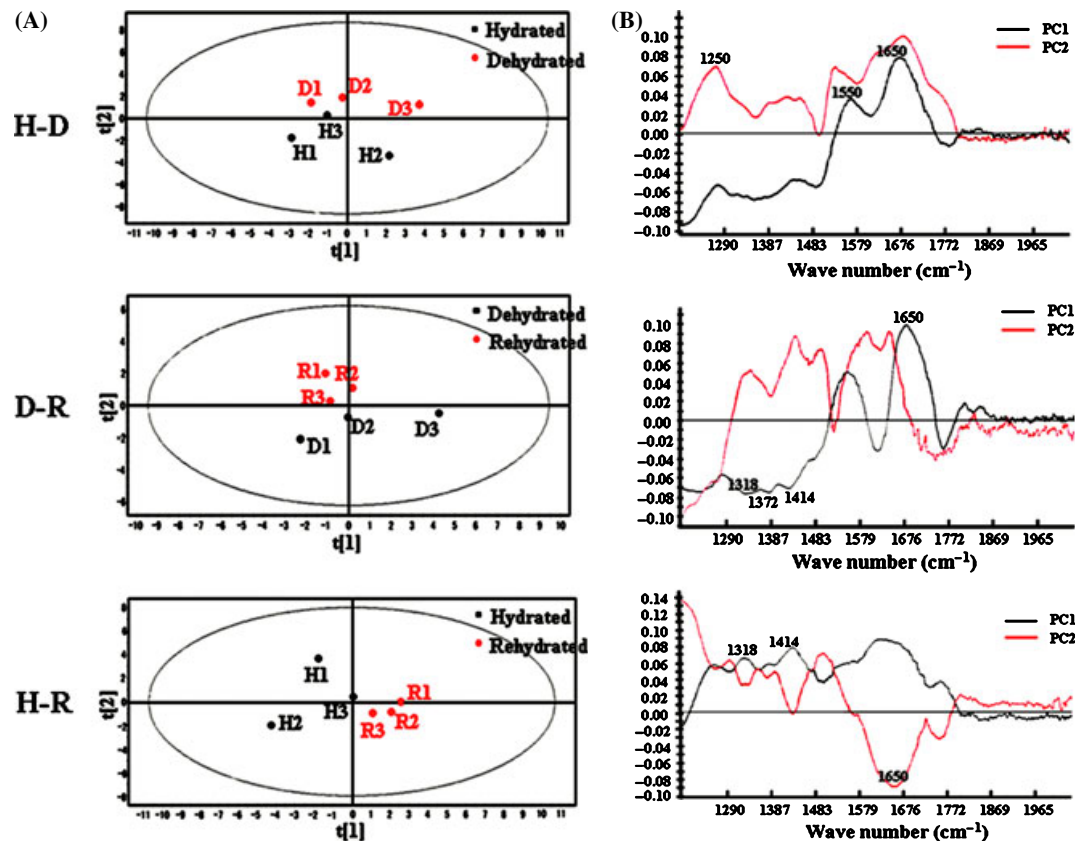


**Fig. 7.** PCA plots of FTIR spectra of cell wall composition changes as a result of dehydration and rehydration. Scores plots (A) and the corresponding loadings plots (B) from PCA classifying hydrated and dehydrated (H–D), dehydrated and rehydrated (D–R), hydrated and rehydrated (H–R) samples. Three repetitions for each sample: H1–H3 for hydrated; D1–D3 for dehydrated; R1–R3 for rehydrated.

Our data demonstrates that BhGRP1 belongs to the cell wall-associated GRP class. BhGRP1 transcripts were detectable in hydrated leaves and up-regulated significantly during dehydration (Fig. 2), demonstrating that BhGRP1 is associated with cellular water status and is likely to function in osmotic stress tolerance.

In order to investigate the link between *BhGRP1* and drought-adaptation, structural and compositional analyses of cell wall in response to dehydration and rehydration were performed. Extensive wall folding accompanied with protoplasmic shrinkage was observed in dehydrated *B. hygrometrica* leaf cells. Similar phenomena were reported in other desiccation tolerant plants such as *C. wilmsii* (Thomson & Platt 1997; Vicré *et al.* 1999, 2004; Vander Willigen *et al.* 2003). Folding of the cell wall is thought to prevent the plasma membrane from tearing away from the cell wall (Sherwin & Farrant 1996; Vecchia *et al.* 1998; Farrant *et al.* 1999; Farrant 2000). Cell integrity in *C. wilmsii* and *B. hygrometrica* was confirmed by full recovery of the cell structure and low electrolyte leakage after rehydration (Sherwin & Farrant 1996; Jiang *et al.* 2007). This form of structural adaptation is not exhibited by all desiccation tolerant plant species, for example, in *Xerophyta humilis* no wall folding is observed (Farrant 2000). In contrast, a dehydration induced transition from a large central vacuole to a cluster of smaller vacuoles was proposed to be an adaptation to overcome mechanical stress (Farrant 2000; Proctor *et al.* 2007). In *B. hygrometrica*, both wall folding and smaller vacuoles were observed upon drying, similar to that observed in African desiccation tolerant species including *M. flabellifolius* and *E. nindensis* (Farrant 2000; Vander Willigen *et al.* 2003). Models that describe the inducible responses of the cell wall in *C. wilmsii* and the constitutive factors (wall pectic plasticizers) in the resurrection plant *M. flabellifolia* in response to desiccation have been proposed (Moore *et al.* 2008b).

To gain insight into the changes in chemical composition of the cell wall in *B. hygrometrica* leaves triggered by changes in the relative water content (RWC), FTIR analysis was conducted. FTIR is a technique that has been used to study the chemical composition of plant cell walls (Zeier & Schreiber 1999; Wu *et al.* 2003). In the present study, three major changes in chemical composition in response to water deficit were discovered, namely protein, pectin and wax/suberin content. The increase in protein level was the major change triggered by dehydration in *B. hygrometrica* leaves, whereas the increase of pectin and wax/suberin content occurred mainly during the rehydration phase.

Vicré *et al.* (1999) demonstrated that dehydration induced accumulation of de-esterified pectin in the *C. wilmsii* cell wall. Our results revealed that, compared with the cell wall of untreated leaves, saturated esters and carboxylic acid groups increased in the rehydrated leaf cell wall. These results indicate that both esterified pectin and de-esterified pectin are increased during rehydration in *B. hygrometrica*. The slightly higher peak at  $1414\text{ cm}^{-1}$  suggests that

de-esterified pectin is increased more than the esterified form. The physiological significance of this alteration could be that the carboxyl groups of the de-esterified pectin are able to chelate  $\text{Ca}^{2+}$ , thus enhancing the tensile strength of the cell wall (McCann *et al.* 1994).

Suberization of the stem and leaf surface can affect water transposition and leaf surface wax deposition can be stimulated by changes in water status (Weete *et al.* 1978). The FTIR spectra at different RWC indicate that a cycle of dehydration and rehydration results in an accumulation of wax- or suberin-like aliphatic compounds, supporting a role for suberization as an adaptation mechanism in desiccation tolerance.

Overall protein content was found to increase after dehydration and the protein level was largely maintained upon rehydration (Fig. 6). Extracellular proteins are major components in the cell wall, including both structural proteins and proteins with enzyme activity, either embedded inside or loosely associated to wall matrix (Showalter 1993). The increase in protein may significantly alter the cell wall physical properties, including strength and elasticity that are important to avoid mechanical damages from water loss and refilling during dehydration and rehydration (Jones & McQueen-Mason 2004). Comparison of the scores plots between samples with different water status revealed that the increase of protein level was the major change triggered by desiccation in *B. hygrometrica* leaves. This result provides evidence to support the important role of cell wall proteins in adaptation to desiccation. The maintenance of high protein levels during rehydration infers that cell wall proteins may also be involved in the repair procedure during rehydration, or help to maintain the desiccation-tolerant state for the next round of water deficit. RT-PCR data have shown that *BhGRP1* transcription was induced upon dehydration and remained high during rehydration (Fig. 2). The similarity between the *BhGRP1* expression profile and the cell wall protein increase during dehydration and maintenance during rehydration suggests the involvement of BhGRP1 in cell wall adaptation to water deficit.

Adaptive changes in cell wall protein composition in response to environmental water status are likely to contribute to the maintenance of cell viability. Dehydration responsive genes encoding cell wall proteins have been reported in other resurrection plants and non-resurrection plants (Brett & Waldron 1996; Wu *et al.* 1996; Neale *et al.* 2000; Jones & McQueen-Mason 2004; Huang *et al.* 2008), inferring that cell wall proteins may play a common role in plant responses to drought stress. For example, glycine and proline-rich protein (SDG43c) and small glycine-rich protein (SDG137c) genes were identified in the desiccation tolerant grass *S. stapfianus* (Neale *et al.* 2000) and three  $\alpha$ -expansin genes (*CplExp1/2/3*) were isolated from *C. plantagineum* (Jones & McQueen-Mason 2004). The expression of SDG43c is broadly correlated with a decrease in RWC, whereas a more complex pattern is observed for the  $\alpha$ -expansin genes. *CplExp1* and

*CplExp3* gene expression increased in response to dehydration (Jones & McQueen-Mason 2004). During rehydration, expression of *CplExp3* remained largely unchanged, while expression of *CplExp1* increased as the leaf regained full turgor (Jones & McQueen-Mason 2004). Expansin proteins are proposed to increase wall elasticity or enhance stability, thus contributing to cellular integrity during rapid cellular shrinkage. BhGRP1 represents another dehydration-inducible cell wall structural protein that may specifically associate with the maintenance and repair of the cell walls of resurrection plants during the process of shrinking and expansion in response to dehydration and rehydration.

## ACKNOWLEDGEMENTS

We thank Professor K. Ma, Professor J. Lin and Professor W. Zhang, Institute of Botany, Chinese Academy of Sciences and Professor F. Salamini, Max Planck Institute for Plant Breeding Research Cologne for their excellent discussion, revision and supports on devices and techniques, B. Eilts and C. Yuan for their excellent technical assistance. We thank Professor X. Qi and Ms L. Wang, Institute of Botany, Chinese Academy of Sciences for their enthusiastic help in the PCA analysis of the FTIR data. This project was supported by National Natural Science Foundation of China (No. 30400027) and National High Technology Research and Development Program of China (863 Program) (No. 2007AA021403).

## REFERENCES

- Alonso-Simón A., Encina A.E., García-Angulo P., Álvarez J.M., Acebes J.L. (2004) FTIR spectroscopy monitoring of cell wall modifications during the habituation of bean (*Phaseolus vulgaris* L.) callus cultures to dichlobenil. *Plant Science*, **167**, 1273–1281.
- Altschul S.F., Gish W., Miller W., Myers E.W., Lipman D.J. (1990) Basic local alignment search tool. *Journal of Molecular Biology*, **215**, 403–410.
- Anderson C.M., Wager T.A., Perret M., He Z.H., He D.Z., Kohorn B.D. (2001) WAKs: cell wall-associated kinases linking the cytoplasm to the extracellular matrix. *Plant Molecular Biology*, **47**, 197–206.
- Bellin D., Werber M., Theis T., Weisshaar B., Schneider K. (2002) EST sequencing, annotation and microarray transcriptome analysis identify preferentially expressed genes in sugar beet. *Plant Biology*, **4**, 700–710.
- Bewley J.D. (1979) Physiological aspects of desiccation tolerance. *Annual Review of Plant Physiology*, **30**, 195–238.
- Brett C.T., Waldron K.W. (1996) *The Physiology and Biochemistry of Plant Cell Walls*, 2nd edition. Chapman and Hall, London, UK.
- Chomczynski P., Sacchi N. (1987) Single-step method of RNA isolation acid guanidinium thiocyanate-phenol-chloroform extraction. *Analytical Biochemistry*, **162**, 156–159.
- Deng X., Hu Z.A., Wang H.X. (1999) mRNA differential display visualized by silver staining tested on gene expression in resurrection plant *Boea hygrometrica*. *Plant Molecular Biology Reporter*, **17**, 1–7.
- Deng X., Hu Z.A., Wang H.X., Wen X.G., Kuang T.Y. (2003) A comparison of photosynthetic apparatus of the detached leaves of the resurrection plant *Boea hygrometrica* with its non-tolerant relative *Chirita heterotrichia* in response to dehydration and rehydration. *Plant Science*, **165**, 851–861.
- Deng X., Phillips J., Bräutigam A., Engström P., Johannesson H., Ouwkerk P.B., Ruberti I., Salinas J., Vera P., Iannaccone R., Meijer A.H., Bartels D. (2006) A homeodomain leucine zipper gene from *Craterostigma plantagineum* regulates abscisic acid responsive gene expression and physiological responses. *Plant Molecular Biology*, **61**, 469–489.
- Domingo C., Sauri A., Mansilla E., Conejero V., Vera P. (1999) Identification of a novel peptide motif that mediates cross-linking of proteins to cell walls. *Plant Journal*, **20**, 563–570.
- Farrant J.M. (2000) A comparison of mechanisms of desiccation tolerance among three angiosperm resurrection plant species. *Plant Ecology*, **151**, 29–39.
- Farrant J.M., Cooper K., Kruger L.A., Sherwin H.W. (1999) The effect of drying rate on the survival of three desiccation-tolerant angiosperm species. *Annals of Botany*, **84**, 371–379.
- Hoheisel J.D., Maier E., Mott R., McCarthy L., Grigoriev A.V., Schalkwyk L.C., Nizetic D., Francis F., Lehrach H. (1993) High resolution cosmid and P1 maps spanning the 14 Mb genome of the fission yeast *S. pombe*. *Cell*, **73**, 109–120.
- Huang D., Wu W., Abrams S.R., Cutler A.J. (2008) The relationship of drought-related gene expression in *Arabidopsis thaliana* to hormonal and environmental factors. *Journal of Experimental Botany*, **59**, 2991–3007.
- Jiang G., Wang Z., Shang H.H., Yang W.L., Hu Z.A., Phillips J., Deng X. (2007) Proteome analysis of leaves from the resurrection plant *Boea hygrometrica* in response to dehydration and rehydration. *Planta*, **225**, 1405–1420.
- Jones L., McQueen-Mason S. (2004) A role for expansins in dehydration and rehydration of the resurrection plant *Craterostigma plantagineum*. *FEBS Letters*, **559**, 61–65.
- Kapila J., De Rycke R., Van M.M., Angenon G. (1997) An agrobacterium-mediated transient gene expression system for intact leaves. *Plant Science*, **122**, 101–108.
- Karnovsky M.J. (1965) A formaldehyde-glutaraldehyde fixative of high osmolality for use in electron microscopy. *Journal of Cell Biology*, **27**, 137–139.
- Kumar S., Ramura K., Nei M. (2004) MEGA3: integrated software for molecular evolutionary genetics analysis and sequence alignment. *Briefings in Bioinformatics*, **5**, 150–163.
- Liu X., Wang Z., Wang L.L., Wu R.H., Phillips J., Deng X. (2009) LEA 4 group genes from the resurrection plant *Boea hygrometrica* confer dehydration tolerance in transgenic tobacco. *Plant Science*, **176**, 90–98.

- McCann M.C., Shi J., Roberts K., Carpita N.C. (1994) Changes in pectin structure and localization during the growth of unadapted and NaCl-adapted tobacco cells. *Plant Journal*, **5**, 773–785.
- Meadus W.J. (2003) A semi-quantitative RT-PCR method to measure the *in vivo* effect of dietary conjugated linoleic acid on porcine muscle PPAR gene expression. *Biological Procedures Online*, **5**, 20–28.
- Moore J.P., Nguema-Ona E., Chevalier L., Lindsey G.G., Brandt W.F., Lerouge P., Farrant J.M., Driouich A. (2006) Response of the leaf cell wall to desiccation in the resurrection plant *Myrothamnus flabellifolius*. *Plant Physiology*, **141**, 651–662.
- Moore J.P., Vicré-Gibouin M., Farrant J.M., Driouich A. (2008a) Adaptations of higher plant cell walls to water loss: drought vs desiccation. *Physiologia Plantarum*, **134**, 237–245.
- Moore J.P., Farrant J.M., Driouich A. (2008b) A role for pectin-associated arabinans in maintaining the flexibility of the plant cell wall during water deficit stress. *Plant Signaling and Behavior*, **3**, 102–104.
- Morikawa H., Hayashi R., Senda M. (1978) Infrared analysis of pea stem cell walls and oriented structure of matrix polysaccharides in them. *Plant and Cell Physiology*, **19**, 1151–1159.
- Mousavi A., Hotta Y. (2005) Glycine-rich proteins a class of novel proteins. *Applied Biochemistry and Biotechnology*, **120**, 169–174.
- Neale A.D., Blomstedt C.K., Bronson P., Le T.N., Guthridge K., Evans J., Gaff D.F., Hamill J.D. (2000) The isolation of genes from the resurrection grass *Sporobolus stapfianus* which are induced during severe drought stress. *Plant, Cell and Environment*, **23**, 265–277.
- de Oliveira D.E., Seurinck J., Inze D., Montagu M.V., Botterman J. (1990) Differential expression of five Arabidopsis genes encoding glycine-rich proteins. *Plant Cell*, **2**, 427–436.
- Park A.R., Cho S.K., Yun U.J., Jin M.Y., Lee S.H., Sachetto-Martins G., Park O.K. (2001) Interaction of the Arabidopsis receptor protein kinase Wak1 with a glycine-rich protein, AtGRP3. *Journal of Biological Chemistry*, **276**, 26688–26693.
- Proctor M. (1999) Water-relations parameters of some bryophytes evaluated by thermocouple psychrometry. *Journal of Bryology*, **21**, 263–270.
- Proctor M.C.F., Ligrone R., Duckett J.G. (2007) Desiccation tolerance in the moss *Polytrichum formosum*: physiological and fine-structural changes during desiccation and recovery. *Annals of Botany*, **99**, 75–93.
- Reichel C., Mathur J., Eckes P., Langenkemper K., Koncz C., Schell J., Reiss B., Maas C. (1996) Enhanced green fluorescence by the expression of an *Aequorea victoria* green fluorescent protein mutant in mono- and dicotyledonous plant cells. *Proceedings of the National Academy of Sciences of the United States of America*, **93**, 5888–5893.
- Reynolds E.S. (1963) The use of lead citrate at high pH as an electron-opaque stain in electron microscopy. *Journal of Cell Biology*, **17**, 208–212.
- Ringli C., Keller B., Ryser U. (2001) Glycine-rich proteins as structural components of plant cell walls. *Cellular and Molecular Life Sciences*, **58**, 1430–1441.
- Sachetto-Martins G., Franco L.O., de Oliveira D.E. (2000) Plant glycine-rich proteins: a family or just proteins with a common motif? *Biochimica et Biophysica Acta*, **1492**, 1–14.
- Sherwin H.W., Farrant J.M. (1996) Differences in rehydration of three desiccation-tolerant angiosperm species. *Annals of Botany*, **78**, 703–710.
- Showalter A.M. (1993) Structure and function of plant cell wall proteins. *Plant Cell*, **5**, 9–23.
- Spurr A.R. (1969) A low-viscosity epoxy resin embedding medium for electron microscopy. *Journal of Ultrastructure Research*, **26**, 31–43.
- Sutherland G.B. (1952) Infrared analysis of the structure of amino acids, polypeptides and proteins. *Advances in Protein Chemistry*, **7**, 291–318.
- Thomson W.W., Platt K.A. (1997) Conservation of cell order in desiccated mesophyll of *Selaginella lepidophylla* ([Hook and Grev.] Spring). *Annals of Botany*, **79**, 439–447.
- Vander Willigen C., Pammenter N.W., Jaffer M.A., Mundree S.G., Farran J.M. (2003) An ultrastructural study using anhydrous fixation of *Eragrostis nindensis*, a resurrection grass with both desiccation-tolerant and -sensitive tissues. *Functional Plant Biology*, **30**, 281–290.
- Vecchia F.D., Asmar T.E., Calamassi R., Rascio N., Vazzana C. (1998) Morphological and ultrastructural aspects of dehydration and rehydration in leaves of *Sporobolus stapfianus*. *Plant Growth Regulation*, **24**, 219–228.
- Vicré M., Sherwin H.W., Driouich A., Jaffer M.A., Farrant J.M. (1999) Cell wall characteristics and structure of hydrated and dry leaves of the resurrection plant *Craterostigma wilmsii*, a microscopical study. *Journal of Plant Physiology*, **155**, 719–726.
- Vicré M., Lerouxel O., Farrant J., Lerouge P., Driouich A. (2004) Composition and desiccation-induced alterations of the cell wall in the resurrection plant *Craterostigma wilmsii*. *Physiologia Plantarum*, **120**, 229–239.
- Weete J.D., Leek G.L., Peterson C.M., Currie H.E., Branch W.D. (1978) Lipid and surface wax synthesis in water-stressed cotton leaves. *Plant Physiology*, **62**, 675–677.
- Wu Y.J., Sharp R.E., Durachko D.M., Cosgrove D.J. (1996) Growth maintenance of the maize primary root at low water potentials involves increases in cell-wall extension properties, expansin activity, and wall susceptibility to expansins. *Plant Physiology*, **111**, 765–772.
- Wu X.Q., Lin J.X., Zhu J.M., Hu Y.X., Hartmann K., Schreiber L. (2003) Casparian strips in needles of *Pinus bungeana*: isolation and chemical characterization. *Physiologia Plantarum*, **117**, 421–424.
- Zeier J., Schreiber L. (1999) Fourier transform infrared-spectroscopic characterization of isolated endodermal cell walls from plant roots: chemical nature in relation to anatomical development. *Planta*, **209**, 537–554.